JPEDAV (2009) 30:595–601
DOI: 10.1007/s11669-009-9582-2
1547-7037 ©ASM International

Experimental Investigation of the Zn-Al-Sb System at 450 °C

Zhongxi Zhu, Xuping Su, Fucheng Yin, Jianhua Wang, and Changjun Wu

(Submitted March 30, 2009; in revised form June 29, 2009)

An isothermal section of the Zn-Al-Sb ternary system at 450 °C has been established by equilibrating 11 samples of different compositions and phase identification by optical and scanning electron microscopy with energy dispersive spectroscopy, x-ray diffraction after quenching to room temperature. Five three-phase regions exist in the system at 450 °C. No ternary compound has been found. And, the compound AlSb with 2.1 at.% Zn can equilibrate with all phases in the system. Experimental results indicate that the solubility of Sb in α-Al phase is too limited to be detected. The SbZn, Sb_2Zn_3, and Sb_3Zn_4 phases, which have little Al solubility (at most 3.3 at.%), were observed in the system.

Keywords phase diagram, phase equilibrium, x-ray diffraction, Zn-Al-Sb

1. Introduction

Hot-dip galvanizing is an effective and economic means against atmospheric corrosion for steel parts. The bath additive elements have a great effect on the structure and the surface quality of the coating. Aluminum is the most important element in galvanizing and different Al levels are required to produce different types of coatings,[1] i.e., 0.024 at.% Al for general galvanizing, about 0.48 at.% Al for continuous galvanizing, 11.2 at.% Al for galfan and 74.63 at.% Al for galvalume. Therefore, the Zn-Fe-Al system is one of the most important systems in studying of zinc-coated steel and has been well studied.[2-4]

Pb is another excellent bath additive element for improving the fluidity of molten zinc, the formation of spangle, the development of excellent microstructure, and the protection of the bath pot.[5] However, it has been prohibited because of its toxicity. Sb is an avirulent element which shows good promise for replacing Pb in galvanizing. Sb has similar function with Pb in a zinc bath[6] which not only makes the molten zinc more fluid and promotes the formation of spangle,[7] but also has a very low segregation coefficient and a correspondingly high solute concentration in the melt at the interface.[8] Pb and Sb have been widely used in continuous galvanizing, and an increase in antimony content does not change the crystal texture or the brightness. That is even better than the addition of Pb. Furthermore, Chang and Shin[7] reported that the solid solution or compound formation in the Sb-Al system should lower the activity of Al in the grain boundaries and reduce the intergranular corrosion when formed in the coating if the bath contains Sb and Al at the same time. At present, different amounts of Sb are added to the bath,[9,10] and amounts in the range 0.01 to 0.27 at.% are often used.[11]

Generally, the hot-dip galvanizing processing is performed at 450 °C. When Sb is added into the Al-containing zinc bath, the bath essentially becomes a Zn-Fe-Al-Sb quaternary system. To fully understand the effect of Sb on the galvanizing process, knowledge of phase equilibrium in the quaternary system at 450 °C is needed. However, until now, there has been no information about phase equilibria of the Zn-Al-Sb ternary system in the literature. The main purpose of this study, which constitutes part of the authors' endeavor to determine the Zn-rich corner of the Zn-Fe-Al-Sb quaternary system, was to experimentally investigate the phase equilibria of Zn-Al-Sb system at galvanizing temperature.

2. Available Information About the Binary Systems

The Al-Zn system is an eutectic system involving a monotectoid reaction and a miscibility gap in the solid state.[12,13] Although it has been studied time and again, there are still some uncertainties with regard to the position of the α-Al phase boundary. So the liquidus curve of the α phase has been repeatedly determined.[14,15] Ellwood[16] determined the solidus curve of the α phase with high-temperature x-ray analysis. The low-temperature solubility was linear extrapolations of experimental data obtained by Auer and Mann[17] and Loehberg.[18] The solubility limits in the assessed phase diagram were based on resistivity measurement data of Fink[19] and Larsson.[20] However, the phase boundaries in the prevailing Zn-Al phase diagram were still drawn based on early microscopic studies.[21,22]

Zhongxi Zhu, Xuping Su, Fucheng Yin, Jianhua Wang, and **Changjun Wu**, Key Laboratory of Materials Design and Preparation Technology of Hunan Province, Xiangtan, Hunan, P.R. China and School of Mechanical Engineering, Xiangtan University, 411105 Xiangtan, Hunan, P.R. China. Contact e-mail: sxping@xtu.edu.cn.

Table 1 Crystallographic data of the binary compounds in the Zn-Al-Sb ternary system

Compound	Crystal system	Pearson	Space group	Lattice parameters (nm)			Reference
				a	*b*	*c*	
ZnSb	orthorhombic	*oP*16	$P2_1/b2_1/c2_1/a$ (61)	0.6218	0.7741	0.8115	[26]
Sb_3Zn_4	trigonal	*hR*22	$R\bar{3}2/c$ (167)	1.2233	1.2233	1.2428	[27]
Sb_2Zn_3	monoclinic	*mS*44	*C*12/c1 (15)	1.074	1.22	0.82	[28]
AlSb	cubic	*cF*8	$F\bar{4}3m$ (216)	0.6135	0.6135	0.6135	[36]

Three recent assessments[23-25] of the Sb-Zn system have been made. Three compounds of SbZn, Sb_3Zn_4, and Sb_2Zn_3 were observed. Crystallographic data for the three compounds[26-28] are listed in Table 1. It needs to be mentioned that there exist high-temperature polymorphic transformations for the Sb_3Zn_4 and Sb_2Zn_3 phases,[29] which were confirmed by Li et al.[24] with a high-temperature XRD determination. Recently, Adjadj et al.[30] proposed a new high-temperature phase Sb_3Zn_4 with a congruent melting and quantitatively determined the homogeneity range of the compound Sb_3Zn_4.

The latest Al-Sb phase diagram has been assessed by Yamaguchi et al.[31] based on a previous study[32] and some new information.[33-35] The system is a simple phase diagram with two eutectic points and just one intermediate compound, AlSb, with the cubic ZnS structure[36] (Table 1) and with a congruent melting point at 1058 °C.[31] There is no evidence in the literature for mutual solid solubility between Al and Sb.

3. Experimental

The compositions of the prepared alloys are listed in Table 2. All alloys were prepared with metals of 99.99 at.% purity. Samples were prepared by carefully weighing Al, Zn, and Sb pellets, 4 g in total for each sample. All masses were weighed to an accuracy of 0.0001 g. The three kinds of metals were mixed and then put into corundum crucibles that were then sealed in evacuated quartz capsules. Each sample was heated to a temperature above its estimated liquidus temperature and kept at this temperature for 20 h. This was followed by quenching in water using a bottom-quenching technique[37] to minimize Zn loss and to reduce sample porosity. The quenched samples were then sealed again individually in evacuated quartz tubes. All samples were then introduced into a furnace kept at 450 °C for 30 days. The samples were water quenched at the end of the treatment.

The specimens were prepared in the conventional way for microstructure examination. A nital solution was used to reveal the microstructures of the samples. Conventional optical microscopy was used for the examination of all the specimens. The phase identification and the chemical composition determination of all phases were performed in a JSM-6360LV scanning electron microscope (SEM) equipped with energy dispersive x-ray spectroscopy (EDS). Furthermore, the phase makeup of the alloys was further determined by analyzing XRD patterns generated by a BEVKER-AXS/D8ADVANCE x-ray diffractometer with Cu Kα-radiation.

Table 2 Composition of specimens and phases in the Zn-Al-Sb ternary system (at.%)

Alloy	Design composition	Phase	at.% Sb	at.% Zn	at.% Al
A1	4Sb-85Zn-11Al	AlSb	47.5 ± 0.5	2.1 ± 0.2	50.4 ± 0.5
		η	···	92.5 ± 0.5	7.5 ± 0.5
A2	11Sb-85Zn-4Al	η	2.2 ± 0.5	95.8 ± 0.5	2.0 ± 0.5
		AlSb	47.2 ± 0.5	1.3 ± 0.2	51.5 ± 0.5
		Sb_2Zn_3	44.4 ± 0.5	55.1 ± 0.5	0.5 ± 0.1
A3	38Sb-57Zn-5Al	η	2.8 ± 0.5	96.0 ± 0.5	1.2 ± 0.5
		AlSb	49.3 ± 0.5	1.5 ± 0.2	49.2 ± 0.5
		Sb_2Zn_3	44.6 ± 0.5	54.9 ± 0.5	0.5 ± 0.1
A4	40Sb-57Zn-3Al	Sb_3Zn_4	45.6 ± 0.5	52.0 ± 0.5	2.4 ± 0.2
		Sb_2Zn_3	43.3 ± 0.5	56.3 ± 0.5	0.4 ± 0.1
		AlSb	50.2 ± 0.5	1.2 ± 0.2	48.6 ± 0.5
A5	49Sb-31Zn-20Al	AlSb	47.4 ± 0.5	1.5 ± 0.2	51.1 ± 0.5
		α-Sb	100	···	···
		SbZn	52.5 ± 0.5	47.5 ± 0.5	···
A6	47Sb-43Zn-10Al	SbZn	54.1 ± 0.5	45.9 ± 0.5	···
		Sb_3Zn_4	45.2 ± 0.5	52.1 ± 0.5	2.7 ± 0.2
		AlSb	51.7 ± 0.5	1.0 ± 0.1	47.3 ± 0.5
A7	46Sb-44Zn-10Al	SbZn	52.6 ± 0.5	47.4 ± 0.5	···
		Sb_3Zn_4	46.8 ± 0.5	50.1 ± 0.5	3.1 ± 0.2
		AlSb	51.1 ± 0.5	1.5 ± 0.2	47.4 ± 0.5
A8	45Sb-45Zn-10Al	SbZn	51.5 ± 0.5	48.5 ± 0.5	···
		Sb_3Zn_4	46.1 ± 0.5	50.8 ± 0.5	3.1 ± 0.2
		AlSb	50.8 ± 0.5	2.0 ± 0.2	47.2 ± 0.5
A9	48Sb-42Zn-10Al	AlSb	51.1 ± 0.5	1.9 ± 0.2	47.0 ± 0.5
		SbZn	52.6 ± 0.5	47.4 ± 0.5	···
A10	3Sb-57Zn-40Al	AlSb	47.8 ± 0.5	0.5 ± 0.2	51.7 ± 0.5
		η	···	69.4 ± 0.5	30.6 ± 0.5
		α-Al	···	42.1 ± 0.5	57.9 ± 0.5
A11	3Sb-17Zn-80Al	AlSb	47.3 ± 0.5	0.3 ± 0.1	52.4 ± 0.5
		α-Al	···	8.7 ± 0.2	91.3 ± 0.5

4. Results and Discussion

In general, different phases react with the etchant to different degrees thereby resulting in different depth of etching. Thus, phases can be easily differentiated based on the level of etching and the chemical compositions were analyzed using the SEM-EDS technique. Furthermore, the true identities of the phases were identified by XRD. All phases found

in the alloys are listed in the Table 2 (Column 3) together with the average chemical compositions (Columns 4-6) of at least five measurements by the SEM-EDS technique.

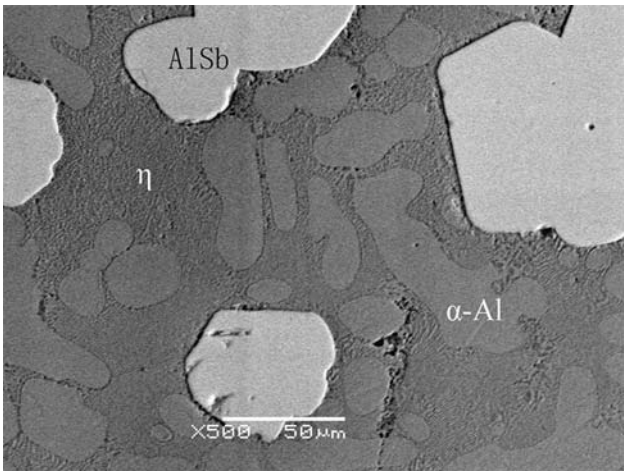

Fig. 1 The back scattered electrons (BSE) micrograph of A1 (4Sb-85Zn-11Al) shows that the liquid is in equilibrium with AlSb at 450 °C

Specimens A1 and A2 are located in the Zn-rich corner of the system. The microstructure of specimen A1 (4Sb-85Zn-11Al) is shown in Fig. 1. Three phases, AlSb, η, and α-Al, were observed. However, in fact, η and α-Al formed when the liquid was water quenched from 450 °C. There is equilibrium of AlSb and η at 450 °C at compositions of specimens A1 and A2. The EDS results show that 2.1 at.% Zn was dissolved in the AlSb compounds, and 7.5 at.% Al was detected in the liquid phase while no Sb was dissolved in it.

The designed compositions of A2 (11Sb-85Zn-4Al) and A3 (38Sb-57Zn-5Al) are located in the three phases region, Sb_2Zn_3, AlSb, and η, as shown in Fig. 2(a, b), which were confirmed by x-ray diffraction pattern (Fig. 2c). It should be mentioned that the η-Zn, which is marked in the figure, is the liquid phase stably existing at 450 °C and apparently supersaturated with Al when the liquid is cooled quickly from 450 °C. The appearance of these two pictures seems much different because the A2 is located in Zn-rich region while the A3 is Sb_2Zn_3-rich. However, their morphologies are same after etching. A small amount of Zn-rich dendrites precipitate during quenching from liquid, these can be observed in Fig. 2(a). On the other hand, only 0.5 at.% Al is dissolved in the Sb_2Zn_3 phase.

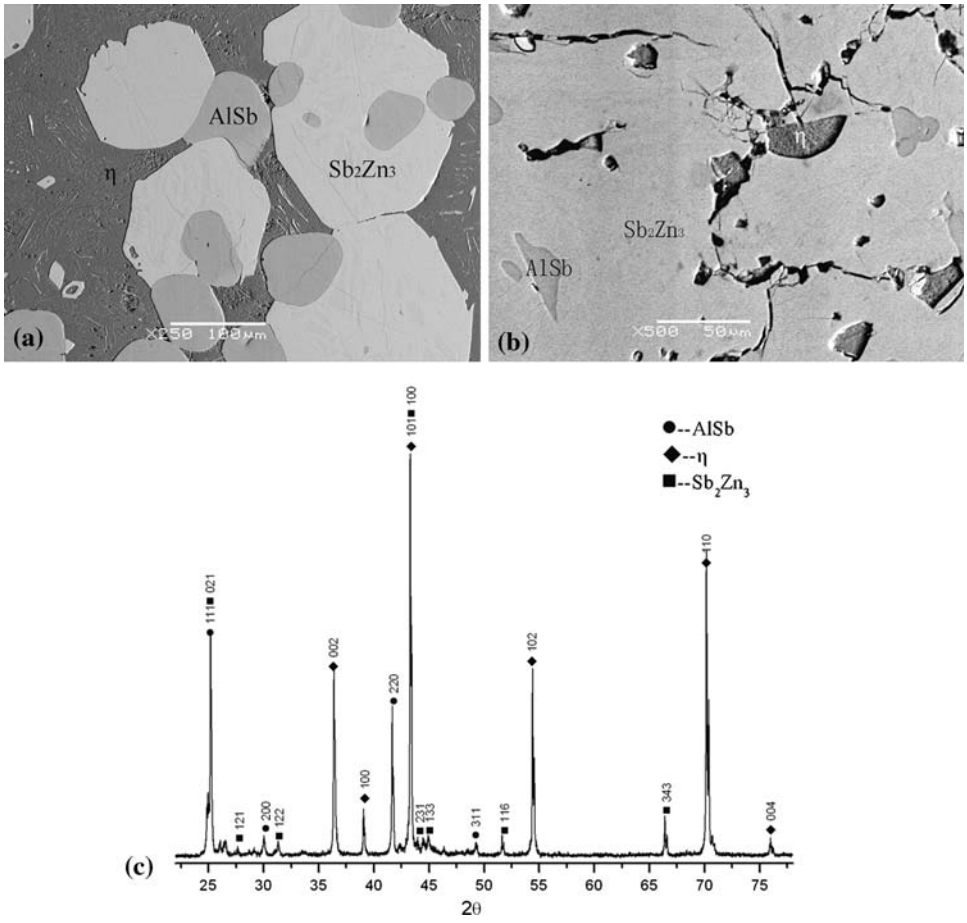

Fig. 2 The three phases region of Sb_2Zn_3, AlSb and η observed from BSE micrograph of specimens (a) liquid-rich A2 (11Sb-85Zn-4Al) and (b) Sb_2Zn_3-rich A3(38Sb-57Zn-5Al). (c) The x-ray powder diffraction pattern of A2

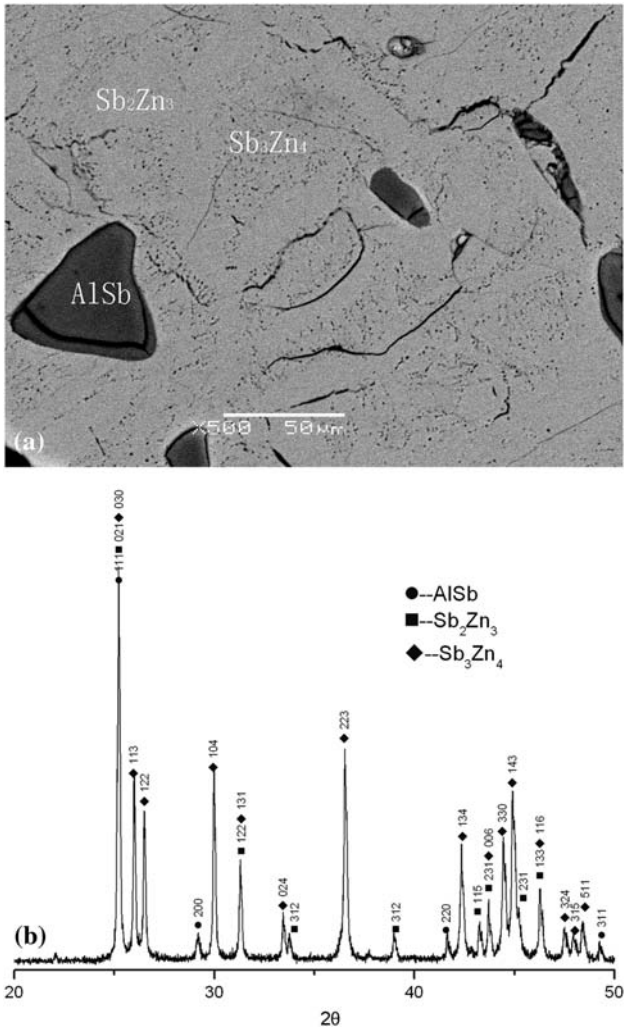

Fig. 3 (a) The BSE micrograph of A4 (40Sb-57Zn-3Al) indicates it consists of three phases, Sb_3Zn_4, Sb_2Zn_3, and AlSb. (b) X-ray powder diffraction pattern of A4 (40Sb-57Zn-3Al) indicates it consists of three phases, Sb_3Zn_4, Sb_2Zn_3, and AlSb

The specimen A4 (40Sb-57Zn-3Al) consists of three phases, Sb_3Zn_4, Sb_2Zn_3, and AlSb, which were confirmed by microstructure (Fig. 3a) and x-ray powder diffraction pattern (Fig. 3b). Because the compounds Sb_2Zn_3 and Sb_3Zn_4 have vicinal composition and may have similar corrosion resistance to the etchant, the relief of them is too similar to be distinguished. The only way to distinguish them in the micrograph is that there are many holes or dots existing in the Sb_3Zn_4 phase. Thanks to the x-ray analysis, they were clearly distinguished, as shown in Fig. 3(b). The EDS analysis also points out that the compositions of these compounds are close to ideal stoichiometry ratio.

A micrograph of A5 (49Sb-31Zn-20Al) is shown in Fig. 4 and indicates the presence of three phases, AlSb, α-Sb, and SbZn. EDS analyses of this alloy indicate that both the solubility of Al and Zn in the α-Sb phase are negligible. Al is also not dissolved in the SbZn phase.

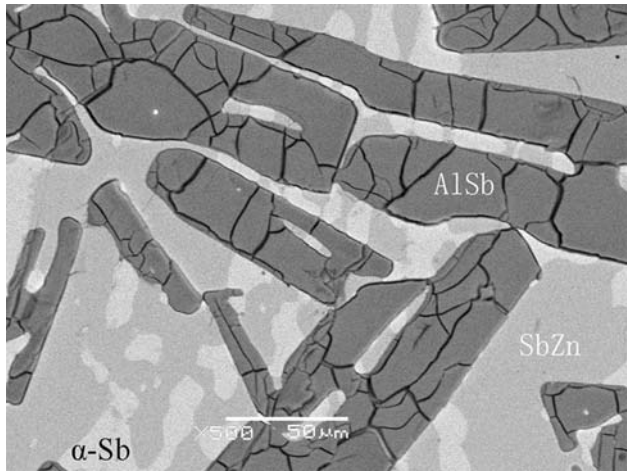

Fig. 4 The BSE micrograph of A5 (49Sb-31Zn-20Al) shows three phases, AlSb, SbZn, and α-Sb

The specimens A6 (47Sb-43Zn-10Al), A7 (46Sb-44Zn-10Al), and A8 (45Sb-45Zn-10Al) contain three phases, Sb_3Zn_4, AlSb, and SbZn. The BSE micrograph of A7 is shown in Fig. 5(a), and its x-ray diffraction pattern is shown in Fig. 5(b). The three phases can be clearly distinguished, although the appearance of SbZn and Sb_3Zn_4 is similar. EDS analyses indicate that the solubility of Al in Sb_3Zn_4 is 3.3 at.% but with no solubility in SbZn when the AlSb compound is in equilibrium with them.

Two phases, SbZn and AlSb, occur in specimen A9 (48Sb-42Zn-10Al). The microstructure of the specimen is shown in Fig. 6. The composition of them also can be found in Table 2. The specimen A10 (3Sb-57Zn-40Al) contains three phases, α-Al, AlSb, and η, as shown in Fig. 7. EDS analyses of this specimen indicate that the solubility of Sb in the α-Al phase is negligible. The equilibrium of α-Al and AlSb was obtained in specimen A11 (3Sb-17Zn-80Al), and it can be clearly observed in Fig. 8.

Based on the SEM-EDS analyses and the x-ray diffraction pattern of the above-mentioned alloys combined with the available information of three binary systems, the phase diagram of the Zn-Al-Sb ternary system at 450 °C was proposed in Fig. 9. The liquid and α-Al two-phase region boundary is drawn based on the existing binary phase diagram and experimental data obtained in this study. The vertices of all three-phase triangles were drawn based on the experimental results obtained in this study.

The compound AlSb, with 2.1 at.% Zn dissolved, can equilibrate with all phases in the system while the Zn-rich liquid phase with the Sb_2Zn_3, AlSb, and α-Al, respectively. From the experimental results, it is clear that the solubility of Sb in α-Al is negligible, and Al and Zn are almost insoluble in the α-Sb, which show an excellent agreement with the binary phase diagram. Furthermore, the Al solubilities in the three Sb-Zn compounds are 3.3 at.% at most and Al was not detected in SbZn in three-phase region α-Sb + AlSb + SbZn.

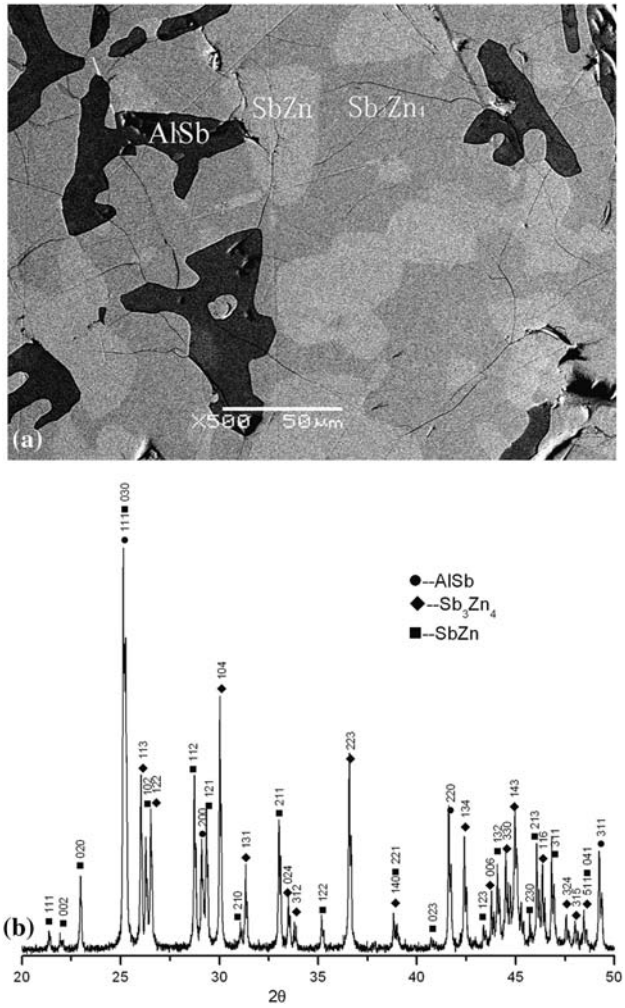

Fig. 5 Specimen A7 consists of three phases, AlSb, SbZn, and Sb_3Zn_4. (a) BSE micrograph. (b) X-ray powder diffraction pattern

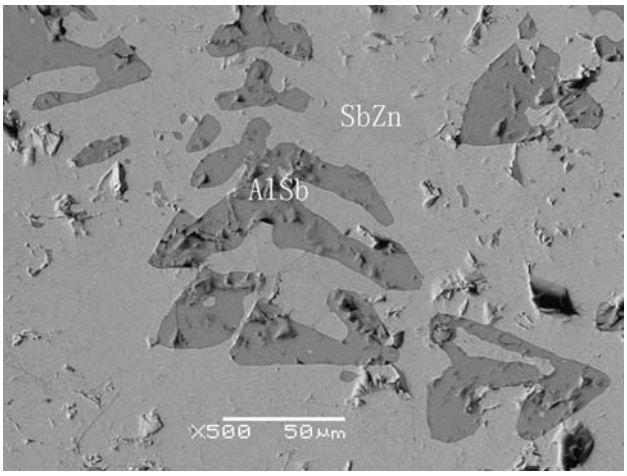

Fig. 6 BSE micrograph of specimen A9 (48Sb-42Zn-10Al) shows two phases, AlSb and SbZn, coexisted

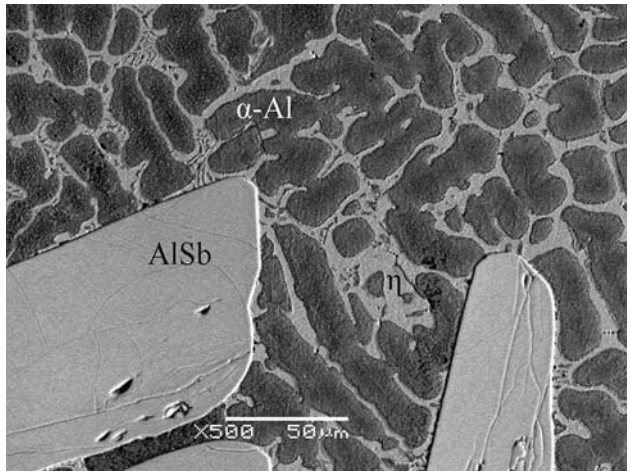

Fig. 7 BSE micrograph of Alloy A10 (3Sb-57Zn-40Al) proves the coexistence of α-Al, AlSb, and η phases

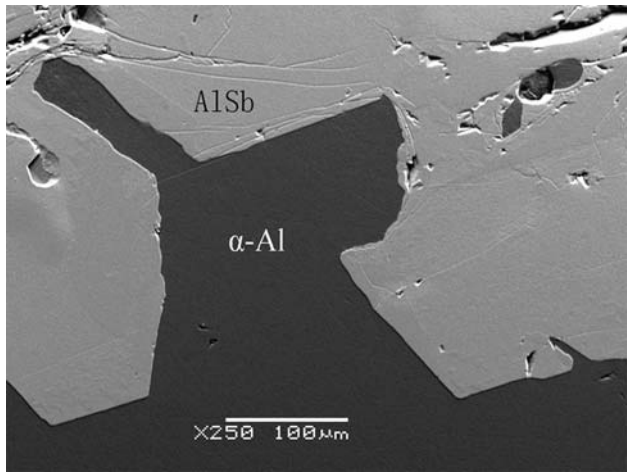

Fig. 8 BSE micrograph of A11 (3Sb-17Zn-80Al) indicates that the α-Al phase coexists with the AlSb phase

5. Conclusions

Based on the microstructures of the alloys and the phase compositions obtained using the SEM-EDS technique, phase equilibrium states available in the Zn-Al-Sb ternary system at 450 °C were determined. There are five three-phase regions and six two-phase regions exist in the system. The compound AlSb can equilibrate with all phases in the system, while the Zn-rich liquid phase can equilibrate with the Sb_2Zn_3, AlSb, and α-Al, respectively. No ternary compound has been found. The EDS results also show that the solubility of Sb in α-Al is negligible which agree well with the binary phase diagram. Furthermore, the Al solubilities in the three Sb-Zn compounds are less than 3.3 at.% and the Zn solubility in the AlSb phase is about 2.1 at.%. However, Al and Zn are almost insoluble in the α-Sb phase.

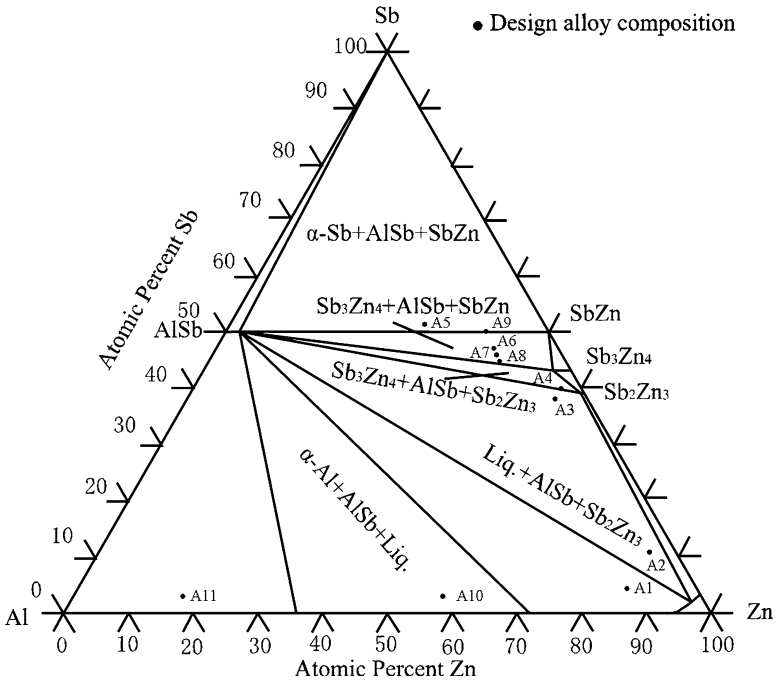

Fig. 9 The 450 °C isothermal section of the Zn-Al-Sb ternary phase diagram. The black dots in the diagram mark the alloy compositions studied in this work

Acknowledgments

This investigation is supported by National Natural Science Foundation of China (Nos. 50671088 and 50771089) and a project supported by Hunan Provincial Science and Technology Department (Nos. 2008WK2001, 2007GK2010, and 2009GK3029).

References

1. A.R. Marder, The Metallurgy of Zinc-Coated Steel, *Prog. Mater. Sci.*, 2000, **45**(3), p 191-271
2. N.-Y. Tang, 450°C Isotherm of Zn-Fe-Al Phase Diagram Update, *J. Phase Equilib. Diff.*, 1996, **17**(5), p 396-398
3. J. Nakano, D.V. Malakhov, S. Yamaguchi, and G.R. Purdy, A Full Thermodynamic Optimization of the Zn-Fe-Al System Within the 420-500°C Temperature Range, *Calphad*, 2007, **31**(1), p 125-140
4. S. Yamaguchi, Equilibrium Phase Diagrams of a Ternary Alloy System of Zn-Fe-Al, *Coating Microstructure and Properties of Galvannealed Steel Sheets,* 2004, p 127-133
5. S. Chang and J.C. Shin, Effect of the Zinc Bath Composition on Hot Dip Galvanized and Galvannealed Steel Sheet, *Galvatech '95 Conference Proceedings*, Chicago, IL, USA, 1995, p 783-786
6. M. Dutta, A. Mukhopadhyay, and S. Chakrabarti, Effect of Galvanising Parameters on Spangle Size Investigated by Data Mining Technique, *ISIJ Int.*, 2004, **44**(1), p 129-138
7. S. Chang and J.C. Shin, The Effect of Antimony Additions on Hot Dip Galvanized Coatings, *Corros. Sci.*, 1994, **36**(8), p 1425-1436
8. J. Strutzenberger and J. Faderl, Solidification and Spangle Formation of Hot-Dip-Galvanized Zinc Coatings, *Metall. Mater. Trans. A*, 1998, **29**(2), p 631-646
9. J. Foct, P. Perrot, and G. Reumont, Interpretation of the Role of Silicon on the Galvanizing Reaction Based on Kinetics, *Scripta Metall. Mater.*, 1993, **28**, p 1195-1200
10. F. Hanna and N. Nassif, Factors Affecting the Quality of Hot-Dip-Galvanized Steel Sheets, *Surf. Tech.*, 1984, **21**(1), p 27-37
11. Y.K. Shindou and M. Kabeya, Zn-Al Hot-Dip Galvanized Steel Sheet Having Improved Resistance Against Secular Peeling of Coating, U.S. Patent 4812371, 1989
12. S.-L. Chen and Y.A. Chang, A Thermodynamic Analysis of the Al-Zn System and Phase Diagram Calculation, *Calphad*, 1993, **17**(2), p 113-124
13. Q.F. Peng, F.S. Chen, B.S. Qi, and Y.S. Wang, Measurement of Al-Zn Phase Diagram by Acoustic Emission During Solidification, *Proceedings of the 95th Annual Meeting of the Transactions of the American Foundrymen's Society*, 1991, p 199-202
14. T. Isihara, On the Equilibrium Diagram of the Aluminum-Zinc System, *Sci. Rep. Tohoku Univ.*, 1925, **13**, p 427-442
15. E. Pelzel, Liquidus and Solidus Curves in Zinc Aluminum System Between 30 and 70% Aluminum, *Z. Metallkd.*, 1949, **40**(4), p 134-136
16. E.C. Ellwood, Solid Solutions of Zinc in Aluminum, *J. Inst. Met.*, 1952, **80**(5), p 217-224
17. H. Auer and K.E. Mann, Magnetic Investigation of Zinc Aluminum System, *Z. Metallkd.*, 1936, **28**(10), p 323-326
18. K. Loehberg, X-ray Determination of Solubility of Aluminum and Copper in Zinc, *Z. Metallkd.*, 1940, **32**(4), p 86-90
19. W. Fink, Equilibrium Relations in Aluminum-Zinc Alloys of High Purity—II, *Trans. AIME*, 1936, **12**, p 244-260
20. L.E. Larsson, Pre-Precipitation and Precipitation Phenomena in Al-Zn Systems, *Acta Metall.*, 1967, **15**(1), p 35-44
21. D. Hanson and L.V. Gayler, *A Further Study of the Alloys of Aluminum and Zinc*, Institute of Metals–Meeting, London, England, 1922, p 1-28
22. E. Gebhardt, Equilibrium Studies of Systems Zinc Aluminum and Zinc Aluminum Copper, *Z. Metallkd.*, 1949, **40**(4), p 136-140

23. X. Liu, C. Wang, I. Ohnuma, R. Kainuma, and K. Ishida, Thermodynamic Assessment of the Phase Diagrams of the Cu-Sb and Sb-Zn Systems, *J. Phase Equilib. Diff.*, 2000, **21**(5), p 432-442
24. J.-B. Li, M.-C. Record, and J.-C. Tedenac, A Thermodynamic Assessment of the Sb-Zn System, *J. Alloys Compd.*, 2007, **438**(1-2), p 171-177
25. L. Zabdyr, A New Thermodynamic Study of the Liquid Sb-Zn and Cd-Sb-Zn Alloys, *J. Phase Equilib.*, 1992, **13**(2), p 130-135
26. F.L. Carter and R. Mazelsky, The Zn-Sb Structure, *J. Phys. Chem. Solid*, 1964, **25**, p 571-581
27. H.W. Mayer, I. Mikhail, and K. Schubert, Some Phases of the Mixtures ZnSbN and CdSbN, *J. Less Common Met.*, 1978, **59**(1), p 43-52
28. G.B. Bokii and R.F. Klevtsova, X-ray Structures Investigation of the Beta-Phase in the Zinc-Antimony, *Zhurnal Strukturnoi Khimii*, 1965, **6**, p 830-834
29. T. Takei, On the Equilibrium Diagram of the Zinc-Antimony System, *Tohoku Imperial Univ. Sci. Rep.*, 1927, **16**(8), p 1031-1056
30. F. Adjadj, E. Belbacha, and M. Bouharkat, Differential Calorimetric Analysis of the Binary System Sb-Zn, *J. Alloys Compd.*, 2007, **430**(1-2), p 85-91
31. K. Yamaguchi, K. Itagaki, and Y. Chang, Thermodynamic Analysis of the In-P, Ga-As, In-As and Al-Sb Systems, *Calphad*, 1996, **20**(4), p 439-446
32. A. McAlister, The Al-Sb System, *J. Phase Equilib.*, 1986, **7**(6), p 522
33. V. Glazov, L. Pavlova, A. Lomov, and E.B. II'Ina, E.m.f. Study of the Thermodynamic Properties of Al-Sb Melts, *Russ. J. Phys. Chem.*, 1992, **66**(5), p 642-645
34. A. Zajaczkowski and J. Botor, Thermodynamics of the Al-Sb System Determined by Vapour Pressure Measurements, *Z. Metallkd.*, 1995, **86**(9), p 590-596
35. K. Yamaguchi, M. Yoshizawa, Y. Takeda, K. Kameda, and K. Itagaki, Measurement of Thermodynamic Properties of Al-Sb System by Calorimeters, *Mater. Trans. JIM*, 1995, **36**(3), p 432-437
36. R.F. Blunt, H.P.R. Frederikse, J.H. Becker, and W.R. Hosler, Electrical and Optical Properties of Intermetallic Compounds. III. Aluminum Antimonide, *Phys. Rev.*, 1954, **96**(3), p 578-580
37. X.-P. Su, N.-Y. Tang, and J. Toguri, 450°C Isothermal Section of the Zn-Fe-Si Ternary Phase Diagram, *Can. Metall. Q.*, 2001, **70**(3), p 377-384